

Dynamic Model of a 7-DOF Whole Arm Manipulator and Validation from Experimental Data

Zaira Pineda Rico, Andrea Lecchini-Visintini and Rodrigo Quian Quiroga

Department of Engineering, University of Leicester, University Road, Leicester, U.K.

Keywords: Whole Arm Manipulator Model, Friction Model, Friction Identification.

Abstract: The present paper describes the design of the dynamic model of a 7 degrees of freedom whole arm manipulator implemented in SimMechanics. The friction phenomena of the manipulator is identified, represented through a fitted model and included in the system model with the aim of increment the accuracy of the model with respect to the real system. The characteristics of the model make it suitable to test and design control strategies for motion and friction compensation in MATLAB/Simulink.

1 INTRODUCTION

The computation of the dynamic model of a robot manipulator plays an important role in simulation of motion, analysis of the manipulator's structure and design of optimal control algorithms. The inclusion of the effects of friction in a mechanical system model when simulating control strategies, helps to improve the performance of the controller to be implemented in the real system (Kostic et al., 2004; Indri, 2006; Bompos et al., 2007). Most of the whole arm manipulators mathematical models are based in the computation of multi-links serial robot's mathematical equations. These equations are obtained using the Newton-Euler recursive method to calculate the Coriolis, centrifugal and inertial forces observed when the end-effector is in motion. Moreover, a Jacobian approach may be implemented in parallel for mapping between Cartesian and joint space, in order to minimize singularity conditions that increase the computation load of the control algorithm (Lau and Wai, 2002; Sousa et al., 2009). This methodology involves both operational and joint forces.

In most cases these mathematical models are implemented using high level computing languages as MATLAB (Corke, 1996), C/C++ or Fortran. Nevertheless, in order to avoid significant computation time, some authors have found in MATLAB/SimMechanics a comfortable tool to design mechanical systems used for experimental verification. The capability of this tool yields appropriate results when working with joints with 1 DOF and when all the manipulator's inertial parameters are known

(MathWorks, 2011).

Section 2 offers a brief description of the real manipulator system. Section 3 gives insights on the design of the model and shows the importance of experimental data in the development of the friction model. In Section 4 the response of the real system is compared to that of the model when simulating some experiments. Finally, section 5 presents some conclusions related to this work.

2 THE REAL SYSTEM

The real system is a 7-degrees-of-freedom whole arm manipulator (WAM) from *Barrett Technology Inc.* It is a joint torque controlled manipulator equipped with configurable PD/PID control and gravity compensation. The information related to the joints configuration, joint motor drives and the body part masses, centre of gravity and inertia matrix is provided by the manufacturer in the WAM ARM User's Manual (Barrett Technology Inc, 2008). Figure 1 shows the configuration and attached frames of the 7-DOF system with a grasper. All the joints of the manipulator are 1 DOF revolute joints. An image of the real system is shown in Figure 2, consisting in a Barret 7-DOF Whole Arm Manipulator with an attached BH8-series BarrettHand.

For the development of this project the 7-DOF manipulator is configured with joint PD control and gravity compensation given by Equation (1), where the joint torque τ is expressed as the sum of the difference

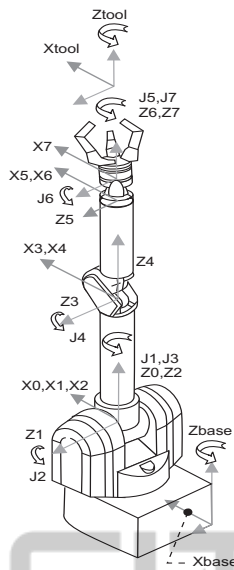


Figure 1: WAM 7-DOF Denavit-Hartenberg architecture with attached frames as shown in (Barrett Technology Inc, 2008).

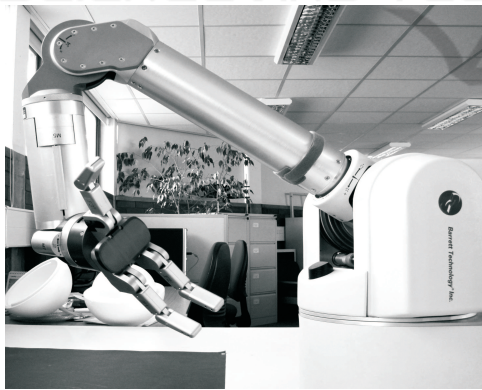


Figure 2: The Barret 7-DOF Whole Arm Manipulator with the BH8-series BarrettHand.

between the reference and measured position, namely position error \tilde{q} , multiplied by a constant proportional gain K_P , the derivative of the error $\dot{\tilde{q}}$ multiplied by a respective derivative gain K_D and the compensation for gravity g , which is a function of the joint position.

$$\tau = K_P \tilde{q} + K_D \dot{\tilde{q}} + g \quad (1)$$

The WAM joint PD control block diagram is shown in Figure 3. The control loop uses the reference signal $r(t)$, namely a joint trajectory, and the measured position $y(t)$ to compute the present error. Then the derivative of the error is calculated, and the gravity compensation is added to conform the joint torque $u(t)$ to be applied to the manipulator's joint.

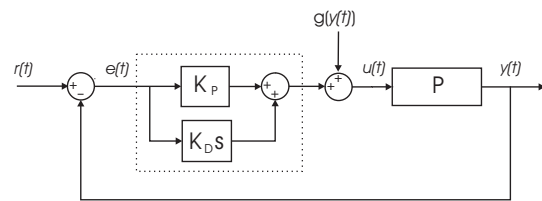


Figure 3: Configuration of the joint PD control with gravity compensation. $r(t)$ is the reference trajectory, $e(t)$ is the response error, P represents the manipulator, $g(y(t))$ is the gravity compensation, K_D and K_P are the derivative and proportional gains, respectively.

3 THE MODEL

The 7-DOF WAM model is built by four blocks:

- Seven modules that compute the joint reference trajectories.
- The dynamic model of the system.
- Fitted friction models for each joint of the manipulator.
- Joint PD controllers configured and tuned as those implemented in the real system.

The dynamic model of the manipulator is based on the configuration and physical characteristics of the real system, the parameters of the friction model are determined through the identification of the joint frictions whilst the joint trajectory and joint controller are emulations of those existent on the real system.

3.1 Trajectory Generation

The reference signal used to perform every joint rotation is a linear segment parabolic blend (LSPB) trajectory defined as follows. Up to a time t_c the trajectory is parabolic with linear velocity, at t_c the trajectory changes to linear with constant velocity and zero acceleration, finally after a time $(t_f - t_c)$ the trajectory changes to parabolic again and the velocity decreases linearly until reaching zero. The motion produced when applying this velocity profile to any joint is translated in a rotation from the initial joint position q_i of the manipulator to q_f radians. Equation (2) defines the described trajectory, where q_i is the initial position, q_f is the final position reached in a time t_f , $\dot{q}_c = \dot{q}_c t_c$ is the value of the constant velocity exhibited from time t_c to time $(t_f - t_c)$ and \ddot{q}_c is the value of the desired constant acceleration.

$$q(t) = \left\{ \begin{array}{ll} q_i + \frac{1}{2} \ddot{q}_c t^2 & 0 \leq t \leq t_c \\ \frac{1}{2} (q_f + q_i - \dot{q}_c t_f) + \dot{q}_c t & t_c < t \leq t_f - t_c \\ q_f - \frac{1}{2} \ddot{q}_c (t_f - t)^2 & t_f - t_c < t \leq t_f \end{array} \right\} \quad (2)$$

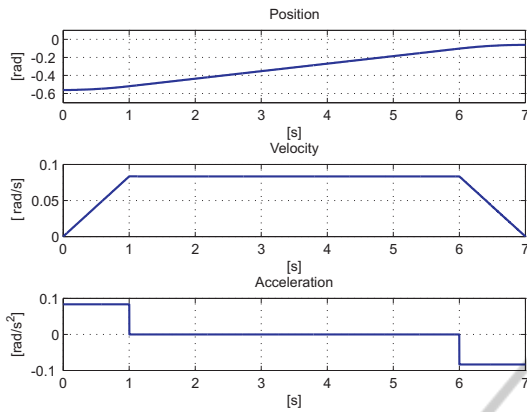


Figure 4: Example of a trapezoidal velocity profile when the values of the variables are set as follows $q_i = -0.55$, $q_f = -0.05$ rads, $\dot{q}_c = 0.083$ rads/s, $t_f = 7$ s and $t_c = 1$.

An example of the trajectory given by Equation (2) can be seen in Figure 4 where a rotation of 0.5 rads is performed.

In order to generate the LSPB joint trajectory, the real system sets the value of the time of change t_c as 1, and the velocity \dot{q}_c and acceleration \ddot{q}_c are calculated using Equations (3) and (4), taking into account the measured values of the initial and the final joint position q_i and q_f .

In simulations, the joint trajectory is emulated by the model considering the experimental values of the initial joint position q_i , the final joint position q_f and the execution time t_f . The value of t_c is set as 1 and the velocity and acceleration are also calculated using Equations (3) and (4). Finally, taking all the parameters previously estimated, the joint trajectory is generated using Equation (2).

$$\dot{q}_c = \frac{4(q_f - q_i)}{t_f^2 - (-2(t_c - 0.5t_f))^2} \quad (3)$$

$$\ddot{q}_c = \dot{q}_c \quad (4)$$

3.2 The Dynamic Model

The dynamic model equation for a robot manipulator is generally written in the form (Siciliano et al., 2009):

$$B(q)\ddot{q} + C(q, \dot{q})\dot{q} + G(q) + F = \tau \quad (5)$$

where q , \dot{q} , \ddot{q} are the position, velocity and acceleration vectors of all the joints that shape the manipulator, $B(q)$ is the inertial matrix, $C(q, \dot{q})\dot{q}$ is the Coriolis-Centrifugal matrix, $G(q)$ is the gravity vector and F is the vector of friction, which is usually obtained using a fitted friction model.

The dynamic model of the WAM Arm was designed and simulated using MATLAB/SimMechanics, and most of the inertial data provided by the manufacturer had to be adapted according to the inertial reference system.

The MATLAB/SimMechanics toolbox is a block diagram modelling environment like Simulink, created by MATLAB, to design and simulate mechanical systems. The toolbox contains several modules that represent particular bodies and which inertial properties can be specified by the user.

A great advantage of using SimMechanics in modelling mechanical systems is that the toolbox is prompt to be used with Simulink so that control routines can be added with ease in order to analyse the behaviour of the system's dynamics under motion constraints.

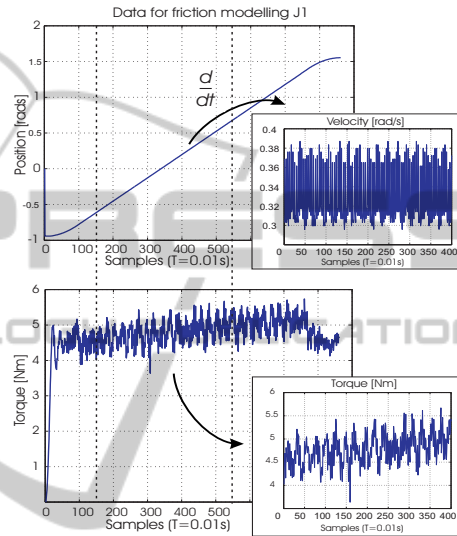


Figure 5: Register of position and torque in the Barret WAM when rotating joint 1 by 0.5 rads.

3.3 The Friction Model

Friction phenomena in robot manipulators may affect the accuracy of the system in position control and when moving the manipulator at very low velocities. Most of the friction models employed when modelling position controlled mechanisms, include several components as the sliding friction (or Coulomb friction), the break-down friction (or stiction) and the viscous friction (Bona and Indri, 2005). In most cases if the manipulator is expected to displace at medium or medium-high velocities, the friction can be expressed mathematically as a function of the joint velocity considering the effects of the viscous friction and the Coulomb friction only (Guran et al., 2001; Lewis et al., 2004; Kelly et al., 2005; Siciliano et al., 2009). This simplified friction model is known as classic friction model:

$$F = F_c \text{sign}(v) + \sigma_2 v \quad (6)$$

where F_c is the parameter for Coulomb friction, σ_2 is the viscous damping coefficient and v is the velocity of the system. The value of the parameters for the classic friction model can be estimated from experimental data

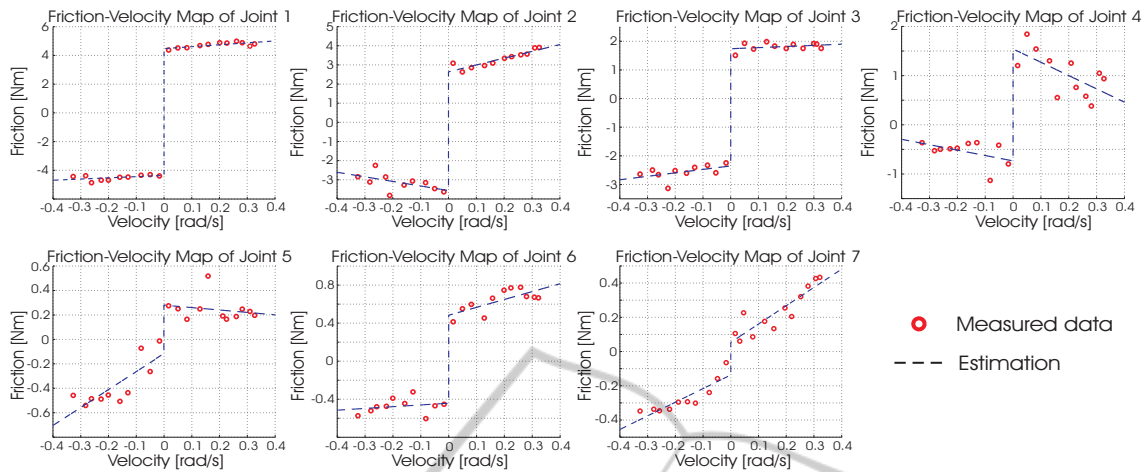


Figure 6: Friction velocity maps corresponding to each joint of the 7 DOF manipulator. The measured data is obtained after rotating each joint of the manipulator at different constant velocities whilst the estimated value is computed using a fitted classic friction model.

through the execution of joint rotations at constant velocity, this process is not straight forward and is explained in detail in section 3.3.1.

3.3.1 Friction Identification

The procedure for the identification of the friction model parameters for each joint of the 7-DOF whole arm manipulator follows several steps. First a closed loop PD control with gravity compensation is used to move the link following a trapezoidal velocity profile at different positive and negative velocities, the measurements of position in addition with the corresponding sampling time are employed to compute the velocity of the link in each experiment. Afterwards, the values of torque and velocity during the constant velocity stage of the trajectory are averaged and used to construct the friction-velocity map, which is basically a torque versus velocity plot. Finally, the parameters for the friction model are estimated to fit the friction-velocity map by applying a least-squares minimization method (Canudas de Wit and Lischinsky, 1997; Canudas de Wit et al., 1995; Olsson et al., 1998; Johnson and Lorenz, 1992) using

$$\sum_{i=1}^n [F(v_i) - \hat{F}(v_i)]^2 \quad (7)$$

where $F(v_i)$ is the measured torque at certain velocity v_i (i.e the friction force), and $\hat{F}(v_i)$ is the value computed by the friction model represented in Equation (6). Figure 5 shows an example of the measured position and torque in the manipulator when rotating joint 1. The data segment in the inset of the figure corresponds to the linear change in the position which is used to compute the joint velocity. The averages of the computed velocity v_i and measured torque $F(v_i)$, respectively, yield to ordered pairs $[F(v_i), v_i]$ that shape the friction velocity map.

The obtained friction model parameters for each

Table 1: Friction model parameters for the seven joints of the robot manipulator. $V+ / V-$ stands for positive and negative velocities respectively.

Joint	Coulomb friction F_c ($V+ / V-$)	Viscous friction σ_2 ($V+ / V-$)
1	4.4748/ 4.3609	1.3348/ 0.8266
2	2.6385/ 3.5643	3.5572/-2.3951
3	1.7399/ 2.3529	0.3944/ 1.2075
4	1.5414/ 0.7342	-2.7045/-1.0969
5	0.2798/ 0.1172	-0.1972/ 1.4670
6	0.4834/ 0.4417	0.8291/ 0.1836
7	0.0538/ 0.1370	1.0689/ 0.7954

joint of the 7-DOF whole arm manipulator are listed in Table 1. There can be noted that the first joint is the most affected by the Coulomb friction F_c whilst the 3 DOF that shape the wrist of the manipulator are the least influenced. These parameters were used to estimate the joint friction velocity maps plotted in Figure 6, where the velocity maps obtained using real data are also shown.

The measured friction suited perfectly the shape of the classic friction model, which reinforces the initial choice of the friction model for the development of this project. In general, the estimation of friction is very accurate for all the joints, and it is suitable enough to be considered when compensating the friction phenomena manifested in the real manipulator.

4 SIMULATIONS

Several joint rotational motion experiments were performed with the aim of evaluate the accuracy of model with respect to the real manipulator. First, a LSPB joint

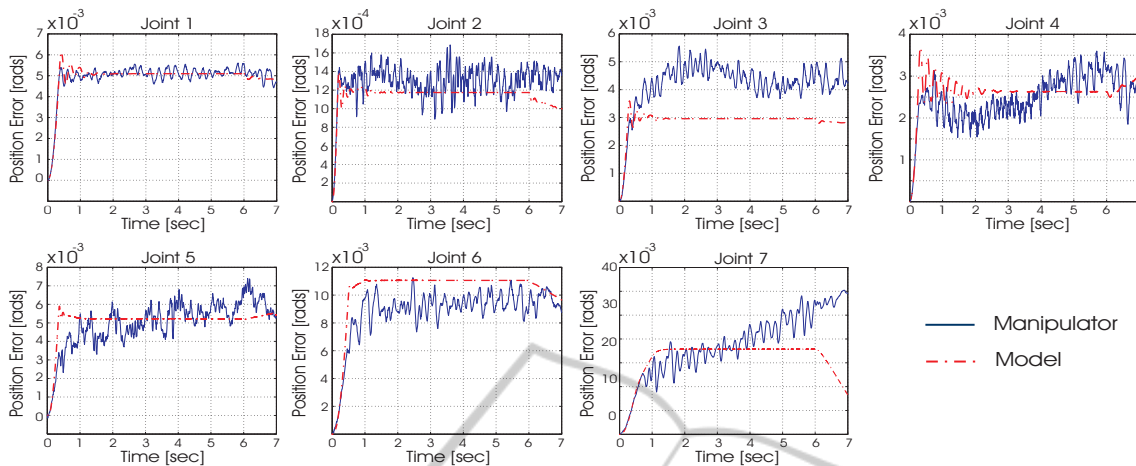


Figure 7: Real and simulated joint error of the 7 DOF manipulator when executing a specific trajectory. Every link is rotated one at a time and the error is calculated using the reference position minus the actual position.

trajectory with a rotation of 0.5 rad at a velocity of 0.083 rads/sec was used as a reference in the real system, and the joint position was measured while the manipulator was in motion. Subsequently, the joint position error was calculated to be used as a performance measurement. Later, in simulation, the same joint trajectory was generated using experimental data as described in Section 3.1. The response of the model was recorded and the model joint position error was calculated.

The position error was chosen as a performance measurement in order to have a closer comparison of the response of both the real manipulator and the model when executing the exact same trajectory. As mentioned earlier, the real system uses a PD control with gravity compensation, and therefore, throughout the simulations a PD control was used and zero gravity was assumed.

During the first set of simulations every link was rotated one at a time. The second set consisted in one simulation only, where all the joints were rotated at the same time. This gave a total of eight simulations performed by the model, to be compared to the behaviour of the real system when executing the exact same trajectory. The graphs in Figure 7 show a comparison of the position error obtained in the first set of simulations. This practice helped to prove the veracity of the model with friction joint per joint and showed that, regardless of the real manipulator is exposed to transducer noise and sensor errors, the response of the model is accurate.

The second set of simulations was more an evaluation of reliability, due to in real exercise the manipulator might operate in Cartesian space and all the joints would rotate at the same time. The response of the model during this simulation was good as expected despite of the clear difference between the simulated and the real position error of the third joint. Figure 8 shows the results of the second set of simulations. The difference in errors between model and real system are expected due to the

disturbances at which the real system is exposed, such as nonlinearities caused by the joint motors and the inertia of the system. Other sources of disturbance to be considered are the joint actuators and the scheme used for gravity compensation.

5 CONCLUSIONS

The identification of friction phenomena in the manipulator is helpful to observe the effects that friction has in the overall performance of the system, so a compensation technique, if necessary according to the application task of the manipulator, may be implemented on the current joint PD/PID control. On the other hand, the inclusion of a friction model in the dynamic model of the mechanical system establish a good platform for simulations in order to observe and analyse the response of the manipulator to different control strategies in a more realistic scenario.

The presented dynamic model with friction is prompt to be used as a reference in the design of joint control strategies implemented in Simulink. By taking advantage of the fact that real joint trajectory is completely emulated in our simulations by setting up the desired rotation angle and execution time, a close comparison of the simulation results with respect to experimental data is also possible.

The development of a dynamic model with friction is extremely useful for observing and improving the performance of the manipulator by analysing the effectiveness of the on system control. In certain cases, some types of stimuli utilised in controller tuning techniques are not feasible to be implemented in experiments whilst the model can be easily manipulated in simulations.

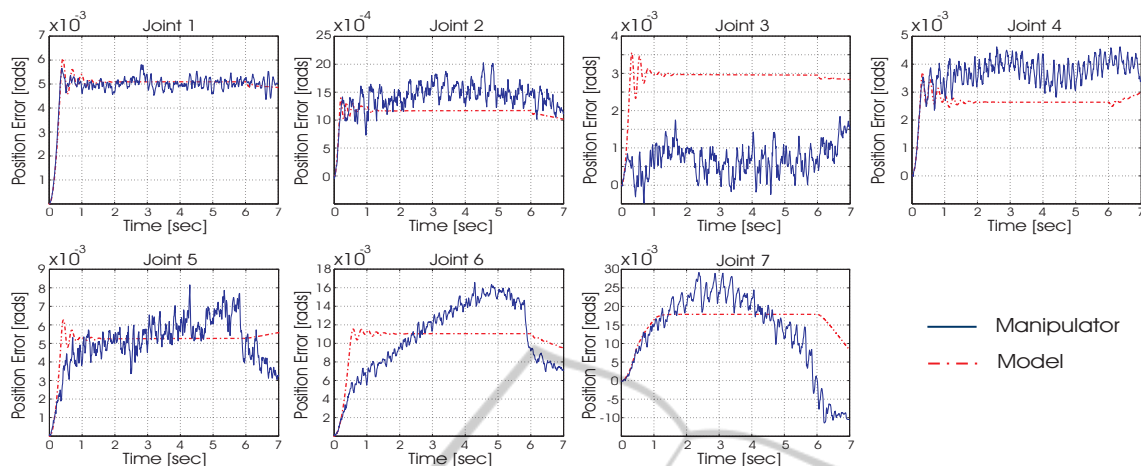


Figure 8: Real and simulated joint error of the 7 DOF manipulator when executing a specific trajectory. All the joints are rotating at the same time and the error is calculated using the reference position minus the actual position.

REFERENCES

- Barrett Technology Inc (2008). *WAM Arm User's Manual*.
- Bompos, N., Artemiadis, P., Oikonomopoulos, A., and Kyriakopoulos, K. (2007). Modeling, full identification and control of the mitsubishi pa-10 robot arm. In *IEEE/ASME International Conference on Advanced Intelligent Mechatronics*.
- Bona, B. and Indri, M. (2005). Friction compensation in robotics: an overview. In *44th IEEE Conference on Decision and Control*.
- Canudas de Wit, C. and Lischinsky, P. (1997). Adaptive friction compensation with partially known dynamic friction model. In *International Journal of Adaptive Control and Signal Processing*.
- Canudas de Wit, C., Olsson, H., Astrom, K., and Lishinsky, P. (1995). A new model for control of systems with friction. In *IEEE Transactions On Automatic Control*.
- Corke, P. (1996). A robotics toolbox for matlab. In *IEEE Robotics and Automation Magazine*.
- Guran, A., Pfeiffer, F., and Popp, K. (2001). Dynamics with friction. In *Series on Stability, Vibration and Control of systems*.
- Indri, M. (2006). Control of manipulators subject to unknown friction. In *45th IEEE Conference on Decision and Control*.
- Johnson, C. and Lorenz, R. (1992). Experimental identification of friction and its compensation in precise, position controlled mechanisms. In *IEEE Transactions on Industry and Applications*.
- Kelly, R., Santibanez, V., and Loria, A. (2005). *Control of Robot Manipulators in Joint Space*. Springer.
- Kostic, D., de Jager, B., Steinbuch, M., and Hensen, R. (2004). Modeling and identification for high performance robot control: An rrr-robotic arm case study. In *IEEE Transactions on Control System Technology*.
- Lau, H. and Wai, L. (2002). A jacobian-based redundant control strategy for the 7-DOF WAM. In *Seventh International Conference on Control, Automation, Robotics and Vision*.
- Lewis, F., Dawson, D., and Abdallah, C. (2004). *Robot Manipulator Control: Theory and Practice*. Marcel Dekker, second edition.
- MathWorks (2011). *MATLAB/SimMechanics*.
- Olsson, H., Astrom, K., Canudas de Wit, C., Gafvert, M., and Lischinsky, P. (1998). Friction models and friction compensation. In *European Journal of Control*.
- Siciliano, B., Sciavicco, L., Villani, L., and Oriolo, G. (2009). *Robotics: Modelling, Planning and Control*. Springer, London.
- Sousa, C., Cortesao, R., and Queiros, P. (2009). Compliant co-manipulation control for medical robotics. In *Proceedings of the 2nd Conference on Human System Interactions*.